Author(s): Benkreira, H.

Title: The effect of substrate roughness on air entrainment in dip coating

Publication year: 2004

Journal title: Chemical Engineering Science

ISSN: 0009-2509

Publisher: Elsevier Ltd.

Publisher's site: *http://www.sciencedirect.com*

Link to original published version: *http://dx.doi.org/10.1016/j.ces.2007.09.045*

The Effect of Substrate Roughness on Air Entrainment in Dip Coating

Hadj Benkreira*

School of Engineering, Design & Technology, University of Bradford, U.K.

Abstract

Dynamic wetting failure was observed in the simple dip coating flow with a series of substrates, which had a rough side and a comparatively smoother side. When we compared the air entrainment speeds on both sides, we found a switch in behaviour at a critical viscosity. At viscosity lower than a critical value, the rough side entrained air at lower speeds than the smooth side. Above the critical viscosity the reverse was observed, the smooth side entraining air at lower speed than the rough side. Only substrates with significant roughness showed this behaviour. Below a critical roughness, the rough side always entrained air at lower speeds than the smooth side. These results have both fundamental and practical merits. They support the hydrodynamic theory of dynamic wetting failure and imply that one can coat viscous fluids at higher speeds than normal by roughening substrates. A mechanism and a model are presented to explain dynamic wetting failure on rough surfaces.

Keywords: Dip Coating - Air entrainment - Dynamic wetting failure- Roughness

* Tel.: +44-1274-233721; fax: +44-1274-235700; *E-mail address*: h.benkreira@bradford.ac.uk

1. Introduction

The principle of coating is to lay a thin film of liquid onto a solid surface. It is a wetting process, which occurs widely in nature and one that has been engineered for a variety of applications, the oldest being painting. Nowadays, there are very few surfaces, which are not coated either for decorative or protective purposes or to add value to them. Magnetic tapes, photographic films and drug patches are three common examples of the modern benefits of coating. In these and most other coating applications, the key requirement of the coating flow is that it must produce a perfectly flat film of uniform thickness (5-100 microns typically) devoid of any defects. The whole coating operation must also be carried out at reasonably high speed (>1 m/s) to be economical. The stumbling block is dynamic wetting failure or the entrainment of air bubbles, which occurs above a critical speed V_{AE}. These air bubbles spoil the quality of the coating, which after drying becomes pitted with craters. As measured by Gutoff and Kendrick (1987) and confirmed by many others (see the authoritative review by Blake and Ruschak, 1997), V_{AE} rapidly decreases with increasing viscosity, μ [V_{AE} (cm/s)=5.11 μ(mPa.s)$^{-0.67}$] and this is also not helpful in practice. Coating liquids by definition are viscous (20 to 1000 mPa.s or more) because they carry solid particles or polymer molecules at high concentration (40% and more) to make subsequent drying not too expensive. Clearly any means of increasing V_{AE} whilst increasing μ (which is partly the aim of this paper) will be most beneficial. To successfully attempt this, one must begin first by understanding the mechanism behind dynamic wetting failure.

Dynamic wetting failure is observed in all coating operations (dip, blade, roll, slide, slot, die, and curtain coating) but its mechanism is best viewed and explained in the simple dip coating flow when a substrate is plunged at a constant speed into a

large pool of liquid. In such a flow and any other coating flows, the free surface of the liquid intersects the solid substrate along the dynamic wetting line and forms with it the dynamic contact angle, θ_D. As the speed of the substrate is increased, the wetting line moves downward and the contact angle increases until it approaches 180^0 at which point the wetting line becomes unsteady and breaks into segments much like the teeth of a saw. At these critical conditions, wetting failure occurs and air bubbles form and are entrained at the tips of the vvv line formed. Figure 1 taken from this experimental programme shows this very clearly. This phenomenon is not new; it has been reported first by Deryagin and Levi (1964) and since then has attracted a lot of research interest (see review by Blake and Ruschak, 1997). Advances have been made in our understanding of the factors that affect V_{AE} but so far we have only been able to quantify the effect of viscosity and lump other effects in the constants of either very basic experimental correlations or complex theoretical equations (see Table 1). The reason for this is that dynamic wetting is a formidable problem and the fundamental question remains unanswered: what is the physical origin of dynamic wetting failure? Is it controlled and can it be modelled by only the hydrodynamic of the system (Voinov 1976 and Cox 1986) or by molecular interactions at the liquid-substrate interface (Blake and Ruschak, 1997). The available data support both approaches in parts but are lacking in helping to develop a new complete theory, which bridges across the two. This paper presents limited but fundamental data to help this development with regard to the effect of substrate roughness which has as yet not been fully evaluated.

Roughness, unlike molecular surface structure, is one surface property, which is easy to create and manipulate, and which a-priori should have a significant effect on V_{AE}. The data of Buonopane, Gutoff and Rimore (1986) suggest that this is the case

with roughness increasing V_{AE} in some tests by a factor as much as 12 in comparison with smooth substrates. These data are however not systematic as the substrates chemistry or porosity were not kept constant. Also, Buonopane, Gutoff and Rimore do not offer experimental mechanistic evidence for this increase in V_{AE} to support the proposition that with rough surfaces, air can escape through the valleys between peaks in the surface. Indeed it is opposite to the received wisdom (Blake and Ruschak, 1997) that roughness should in fact decrease V_{AE} on the basis that the wetting line must move a greater distance across a rough surface than a flat surface of equivalent length. Clearly an explanation is lacking, experimental or theoretical, to reconcile these opposite findings. It is true that Blake and Ruschak (1997) offer an alternative scenario- skipping from peak to peak- as a reason why V_{AE} should increase with roughness. They gave no data to support this view which is based on the theoretical argument that with increasing roughness the wetting line will move a shorter distance causing V_{AE} to increase. The skipping mode however should lead to a dynamic wetting failure different from the classical vvv type. This is because if the liquid skips over the peaks, it will not wet completely the topography of the substrate and small air pockets will be trapped in the intervening valleys. Beyond a critical substrate speed, the air pockets will grow larger than the scale of the roughness, they will get engulfed by the liquid and catastrophic coating failure should ensue rather than the vvv type failure described in Figure 1 in which tiny air bubbles form at the tip of the "v" segments. Clarke (2002) has observed this phenomenon in curtain coating and exploited it to enhance coating speeds by a careful choice of roughness and viscosity. His data at the lowest curtain flow rate show no roughness effect which suggest it may not be observed in dip coating and in other non-assisted hydrodynamically coating flows. We intend to prove that this switch in behaviour –from V_{AE} decreasing to

increasing with increasing roughness- is fundamental to all coating flows when the roughness- flow_(viscosity) conditions are appropriate. It is not peculiar to curtain coating where the skipping over a rough surface is aided by the turning geometry of the impinging curtain and the large coating speeds. In doing so, the present work will complement the observations made at very low wetting speed- with sliding drops- by Menchaca-Rocha (1992), Herminghauss (2000) and Miwa et al. (2000) who also found that as the roughness was increased, drops could move more easily.

2. EXPERIMENTAL METHOD

The dip coater used consists of a 50mm wide vertical tape drawn downwards into and through a transparent tank containing the test liquids to a depth of 150 mm. To cancel edge effects, the tank cross section was 135 mm x 90 mm. The tape was fed from a spool, plunged into the liquid, emerged through a sealed slit at the bottom of the tank and was finally wound around a cylinder driven by a variable speed geared motor. Additional liquid was supplied regularly to the tank to compensate for the amount entrained by the substrate. The tape velocities were measured with an optically triggered digital tachometer mounted on one of the rollers. The onset of the dynamic wetting failure was determined by slowly increasing the tape velocity until the break-up of the wetting line into a saw-teeth pattern could be observed with the naked eye under proper illumination. A digital video camera with a microscopic lens was also used to view and capture images of the flow. Figure 1 shows the dynamic wetting line at break point with its vvv segments. Catastrophic failure was gauged in the same way except that larger bubbles instead of a vvv line would suddenly appear.

In these experiments, 2 non-porous paper and 2 polyester substrates with different roughness on the front (F) and back (B) sides were used. Both the paper and

the polyester substrates were coated with a gelatine sublayer to eliminate differences in their surface molecular structure. Their absolute roughness R_A and average peak-to-valley height roughness R_Z were measured using a PicoForce Multimode Atomic Force Microscope with scan size less than 30 microns and a Taylor Hobson Talysurf 4. The roughnesses obtained from both were consistent as shown in Table 2. We also observed the substrate topography and measured roughness with a MicroXam 3D Interferometric Profiling System (AG ElectroOptics). Again the roughnesses obtained were in par with those of the AFM and Talysurf.

The procedure for measuring the air entrainment speeds was as follows. For any one fluid we observed both the front and back sides of the substrate, increased the speed gradually, measured the air entrainment speed on the side that entrained air first and continued the experiment until the second side showed air entrainment and recorded the corresponding speed. In order to reduce experimental errors, each experiment was repeated at least three times. In spite of the crudeness of the experimental method, the discrepancies between individual and averaged data were always found to be in the range ± 5-10%. All coating experiments were conducted at room temperature (between 20 and 25^{o}C) with glycerol-water solutions. The viscosity of each solution tested was measured before and after the test was carried out at the same temperature in a concentric cylinder viscometer (Brabender Rheotron and Bohlin CVO 120). As expected, the glycerol-water solutions were found to be Newtonian. Depending on the critical viscosity (details later in the results), several solutions were tested covering the range from 50 to 800 mPa.s. The surface tension σ of the fluids and the advancing contact angles θ_D for each pair of fluid-substrate system were measured with a FTA 188 video tensiometer. The difference in wetting behaviour of the paper and polyester substrates is clearly shown in Figure 2 and in the tabulated

values (Table 2) of the contact angles measured immediately after the drop sat on the substrate (t=0) and thirty seconds later (t=30s).

3. RESULTS & DISCUSSION

The important result is the effect of roughness on air entrainment speed above and below a critical viscosity and a critical roughness. When we compared the air entrainment speeds on the rough and smooth side of the paper substrates, we found a switch in behaviour at a critical viscosity. At viscosity lower than a critical value, the rough side entrained air at lower speeds than the smooth side. It also shows the classical vvv failure. Above the critical viscosity the reverse was observed, the rough side entraining air at higher speed than the smooth side. The air entrainment in such a case was sudden and intense and not preceded by a vvv line. This is clearly shown in the flow images of Figure 3. The LHS side shows two sequences at increasing substrate speed for a viscosity of 40 mPa.s. The RHS sequences are for a viscosity of 140 mPa.s. The pattern does not change as we increase the viscosity further. We have the experimental evidence for viscosities up to 800 mPa.s. Hence the assertion that we have for a given substantial roughness a critical viscosity. For this particular roughness (substrate Paper2F, R_Z=3.060 μm), the critical viscosity was found by an iterative experimental procedure to be 84 mPa.s. That is at this viscosity the smooth and the rough sides of this substrate entrained air at exactly the same speed. This is clearly shown in the flow images of Figure 4. This result was confirmed with another paper substrate (Paper1) which also had a smooth and rough side. Its rough side (Paper1F) was however only slightly rougher (R_Z=3.300 μm) than Paper2F, the rough side of Paper2. The resulting effect was that the critical viscosity was larger and measured to be 345 mPa.s, much larger than the 84 mPa.s measured with Paper2F of

R_Z=3.060 μm. The critical viscosity is therefore very sensitive to roughness and a slight increase in it (8%) can push the critical viscosity by a much larger order of magnitude (311%).

This result brings out clearly the importance of hydrodynamic effects- roughness and viscosity- on air entrainment. Only above a critical viscosity is a rough surface more dynamically wetting than a smooth surface. Also, the critical viscosity is pushed to higher value by modest increases in roughness. This is very useful in practice as it implies that higher solid content formulations (higher viscosity) can be coated faster by increasing the roughness of the substrate but not so substantially as to weaken its strength.

When we carried out the experiments with the two polyester substrates Polyester1 and Polyester2, we saw no switch or critical viscosity. In comparison with the paper substrates, these are smoother but they have different roughness on both sides as shown in Table 1. This result together with the results with the paper substrates demonstrate that roughness is only effective in enhancing dynamic wetting when it is large or above a critical value. When we compared V_{AE} with surface Paper1B (R_z=0.600 μm) and surface Paper2B (R_z=1.475 μm), we found again no switch or critical viscosity. This and the data with Paper1F and Paper2F suggest that the critical roughness is in the range 1.5-3 μm. Further experiments with a wider range of roughness on the same type of substrate are needed to delineate more precisely the region in which roughness increases V_{AE}.

The above observation are clearly expressed in the air entrainment speeds data shown in Figures 5-8 for the 4 sides tested together with the correlation of Gutoff and Kendrick (1982). The smooth sides gave air entrainment speeds close to those obtained by Gutoff and Kendrick and this confirms the accuracy of the experimental

technique. The switch at the critical viscosity is clearly shown for the two rough sides, with the rougher side switching at much higher viscosity than the less rough side.

The data clearly demonstrate that depending on the flow conditions (which must include viscosity) and roughness values, roughness could decrease or increase the air entrainment speed. When roughness decreases the air entrainment speed, the air entrainment is of the vvv type and when it increases it, it is of the catastrophic type.

As for the mechanism, skipping from peak to peak is a reasonable explanation for why air entrainment speed should increase with roughness. It also explains the sudden and intense air entrainment at wetting failure. In comparison with curtain coating, the increase in air entrainment speeds is however not very large. Unlike in dip coating, in curtain coating, the liquid impinges on the substrates creating a load pressure that delays the formation of an air film sufficiently larger than the roughness to induce catastrophic wetting failure. Using Blake and Ruschak (1997) approximation of the size h_a of an air film entrained by a smooth substrate travelling at speed V, we have:

$$h_a \approx \frac{\sigma}{P_L}\left[\frac{3\sqrt{2}\pi(1+m)}{8}\left(\frac{\mu_a V}{\sigma}\right)\right]^{2/3} \quad \text{with} \quad m = \frac{1}{1+3\frac{h_a}{L_d}\frac{\mu}{\mu_a}} \qquad (1)$$

P_L is the pressure of the liquid layer L_d onto the air film h_a; σ is the surface tension of the liquid; μ and μ_a are the viscosities of the liquid and the air respectively. We postulate that Equation(1) holds for a rough surface but the air film h_a is taken within the roughness, R_Z. At catastrophic wetting failure, this air film thickness h_a will be just greater than the roughness R_z, the air entrainment velocity will then be:

$$V_{AE} = \left(R_Z \frac{P_L}{\sigma}\right)^{3/2}\left[\frac{8\sigma}{3\sqrt{2}\pi(1+m)\mu_a}\right] \qquad \text{with} \quad m = \frac{1}{1+3\frac{R_Z}{L_d}\frac{\mu}{\mu_a}} \qquad (2)$$

Equation (2) intimates that the roughness effect should be the same in both curtain and dip coating. It would be if both P_L and m were the same. P_L in curtain coating is very large and is due the large kinetic energy of the liquid curtain impinging at speed from the curtain die from a height onto the substrate. It is of order 1000-10,000 Pa. In dip coating, the liquid pressure is much smaller in comparison and of order a few millimetres of water or about 1-10 Pa. This explains why the roughness has such a dramatic effect in curtain coating and a comparatively insignificant effect in dip coating. As for the effect of viscosity, m indicates that it is non-linear and magnified by R_Z/L_d, i.e. roughness. For a given R_Z/L_d, m changes significantly only when the viscosity is large enough to affect the term $1+3\frac{R_Z}{L_d}\frac{\mu}{\mu_a}$. This could explain why roughness becomes effective only at and above a critical viscosity.

4. CONCLUSIONS

This work has provided new experimental evidence of the hydrodynamic origin of dynamic wetting failure. It shows that roughness and viscosity play a critical role and can lead to higher or lower air entrainment speeds. The mechanisms by which the air is entrained also differ. We have shown in particular, that a rough substrate will only coat faster than a smooth substrate when both the roughness and the viscosity exceed a critical value. The critical roughness is only small and according to our data in the range R_Z =1.5-3 μm. The corresponding critical viscosity is 84 mPa.s but increases rapidly with tiny increases in roughness. These results are of practical value as they imply that one can coat viscous fluids at higher speeds than normal by roughening substrates only marginally. Although limited in their range, these key experiments have brought out the essential effect of roughness-viscosity on

dynamic wetting failure in dip coating and by implication other coating flows. These findings consequently provide a firm scientific basis to tune roughness-viscosity to the industrial target of larger V_{AE} with larger viscosities.

Acknowledgements

The author acknowledges the contribution of his Coating Research Team members Dr Raj Patel and Mr Ilyas Khan in the collection of the data. We are also grateful to Dr Olivier Cohu of Ilford Imaging Switzerland GmbH (Marly) for providing the substrates and Dr Russel Evans of AG Electro-Optics UK (Tarporley, Cheshire) for the characterisation of the substrates with the MicroXam 3D.

NOTATION

R_A Absolute roughness

R_Z Average peak-to-valley height roughness

V_{ae} Air entrainment velocity

θ_A Advancing contact angle

θ_D Dynamic contact angle

μ Viscosity

ρ Density

σ Surface tension

REFERENCES

Blake, T.D. (1993). Dynamic Contact Angles and Wetting Kinetics. In Wettability, ed. J. Berg, Chap. 5, p.252. Marcel Dekker, New-York, U.S.A.

Blake, T.D. and Ruschak, K.J. (1997). Wetting: static and dynamic contact lines. In Liquid Film Coating, eds. S.F. Kistler and P.M. Schweizer, Chap. 3, p.63. Chapman & Hall, London, U.K.

Buonoplane, R.A., Gutoff, E.B. and Rimore, M.M.T. (1986). Effect of Plunging Tape Surface Properties on Air Entrainment Velocity. *AIChE J.*, **32**, 682.

Burley, R. and Jolly, R.P.S. (1984). Entrainment of Air into Liquids by a High Speed Continuous Solid Surface. *Chem. Eng. Sci.*, **39**, 1357.

Clarke, A. (2002). Coating on Rough Surface. *AIChE J.*, **48**, 2149.

Cohu, C. and H. Benkreira, H. (1998). Air Entrainment in angled dip coating. *Chem. Eng. Sci.*, **53**, 533.

Cox, R.G. (1986). The dynamics of the spreading of liquids on a solid surface. Part 1. Viscous flow. *J. Fluid Mech.*, **168**, 169.

Deryagin, B.M., and Levi, S.M. (1964). Film Coating Theory, p.137. Focal Press, London, U.K.

Gutoff, E.B. and Kendrick, C.E. (1982). Dynamic Contact Angles. *AIChE J.*, **28**, 459.

Perry, R.T. (1967). Fluid Mechanics of Entrainment through Liquid-Liquid and Liquid-Solid Junctures. PhD Thesis, University of Minnesota, U.S.A.

Voinov, O.V. (1976). Hydrodynamics of wetting. *Fluid Dynamics.*, **11**, 714.

Wilkinson, W.L. (1975). Entrainment of air by a solid surface entering a liquid/air interface. *Chem. Eng. Sci.*, **30**, 1227.

LIST OF FIGURES AND CAPTIONS

Table 1: Experimental and Theoretical Correlations for V_{AE} .

Experimental Correlations with μ in mPa.s and σ in mN/m			
Perry (1967)	U=3.5 μ-0.8	20< μ<300	$\theta_A=70^0$
Perry (1967)	U=6.6 μ-0.73	20< μ<300	$\theta_A=20^0$
Burley and Jolly (1984)	U=0.395(σ/μ)0.77	0.2< σ/μ<3.2	
cellophane, polyester, polypropylene			
Gutoff and Kendrick (1987)	U=5.1 μ-0.67	1< μ<1000	22< σ<72
gelatine-subbed polyester			
Blake (1993)	U=10.7 μ-0.827	1< μ<1000	σ=65
polyethylene terephtalate and gelatine-subbed polyethylene terephtalate			
Wilkinson (1975)	U=0.64σ (μ-0.87)	1< μ<670	σ=65
scraped (damp) rotating steel cylinder			
Cohu and Benkreira (2000):data agree best with Burley and Jolly (1984)			
Theoretical Equations			
Molecular-Kinetic Theory (Blake 1993): $U= (2K_sL_Mh_p/ \mu v) \sinh\{(\sigma/2NkT)(\cos \theta_e- 1)\}$ K_s (frequency of molecular displacement), N (number of adsorption sites per unit area) v (molecular flow volume) and θ_e (static contact angle) need to be determined from experiments. L_M (length of individual displacement)$\approx 1/\sqrt{N}$, h_P (Planck cst), k (Boltzmann cst) and T (absolute temperature)			
Hydrodynamic Theory (Cox 1986): $U\mu/ \sigma = \{(\pi/6) \ln(4\mu/3 \pi \mu_A)-\chi(\theta_W)\}/\ln(L/L_S)$ $\chi(\theta_W)$ (contact angle function), L_S (slip length), L(flow length) need to be determined from experiments. μ_A (air viscosity).			

Table 2: Roughness of substrates used & corresponding Contact Angles with glycerine-water solution of 40 mPa.s

Substrate	**R_A (µm)**	**R_Z (µm)**	**$\theta_{t=0s}$**	**$\theta_{t=30s}$**
Paper1F	0.735	3.300	117.3	110
Paper1B	0.108	0.600	70.5	64.2
Paper2F	0.660	3.060	89.3	86.0
Paper2B	0.305	1.475	65.5	59.2
Polyester1F	0.035	0.185	87.3	60.3
Polyester1B	0.031	0.178	70.5	49.4
Polyester2F	0.039	0.115	77.0	45.3
Polyester2B	0.074	0.230	71.6	44.7

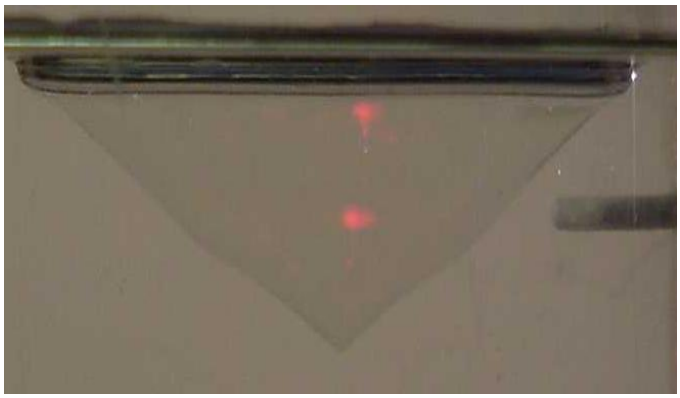

Figure 1: Dynamic wetting failure showing the distinct "V" in the vvv line.

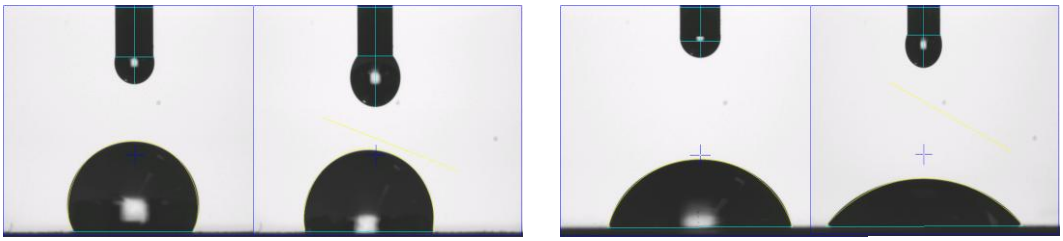

Figure 2: Contact Angles of Paper1 (117^0 to 110^0 after 30s) and Polyester2 (77^0 to 46^0 after 30s).

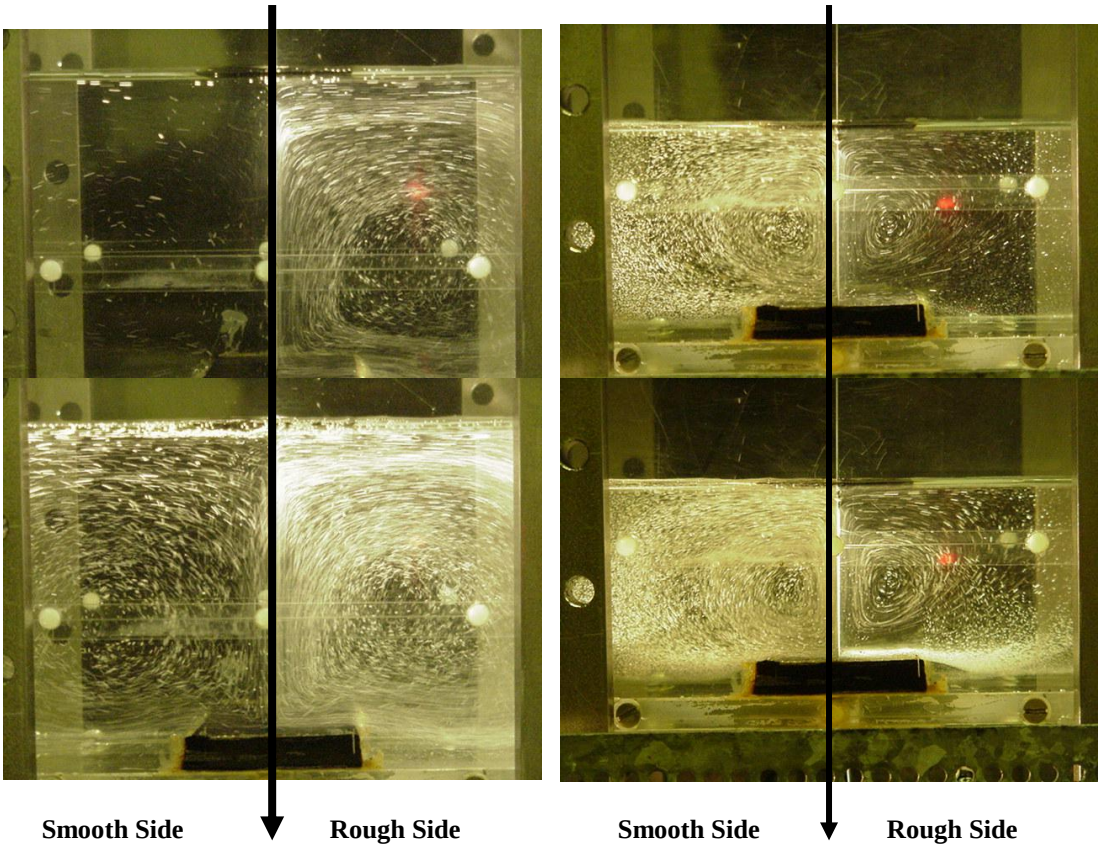

Figure 3: Paper2 Switch in Air Entrainment with Viscosity.
LHS, 40mPa.s. RHS, 140 mPa.s. Note the increased air bubbling as speed is increased beyond wetting failure.

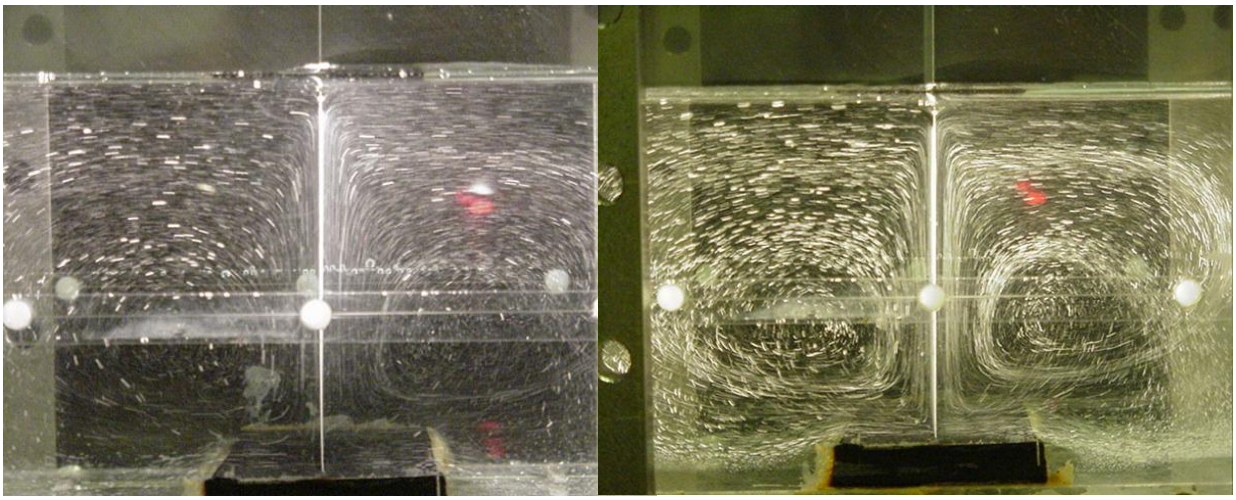

Figure 4: Paper2 Air Entrainment at the Critical Viscosity. Note that as we increase speed (LHS to RHS), the air entrainment is the same on both sides.

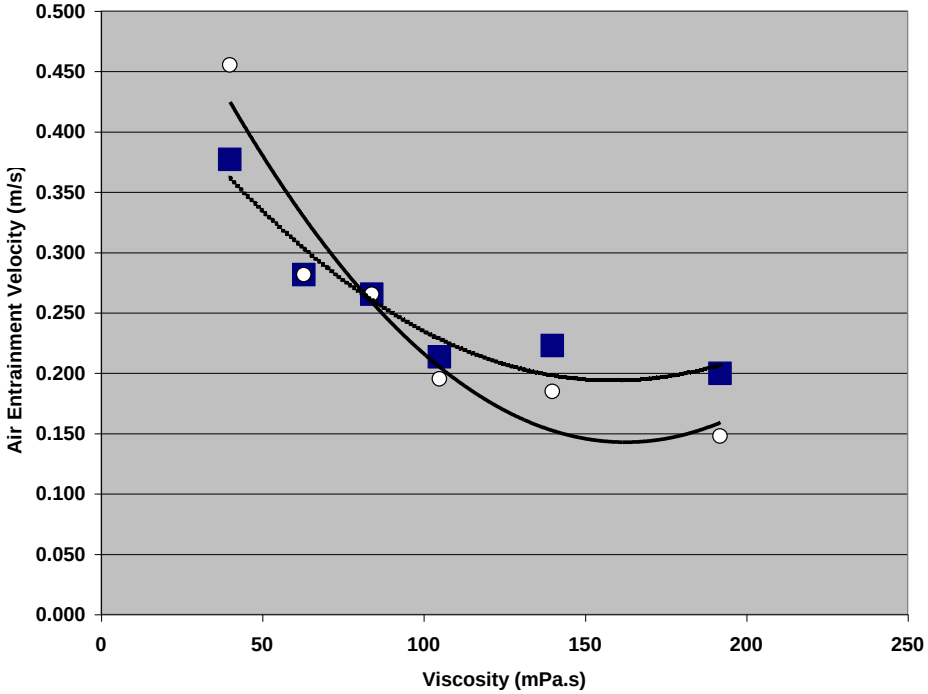

Figure 5: Air Entrainment Speed on the rough (■) and smooth sides (○) of Paper2 showing switch at a low critical viscosity.

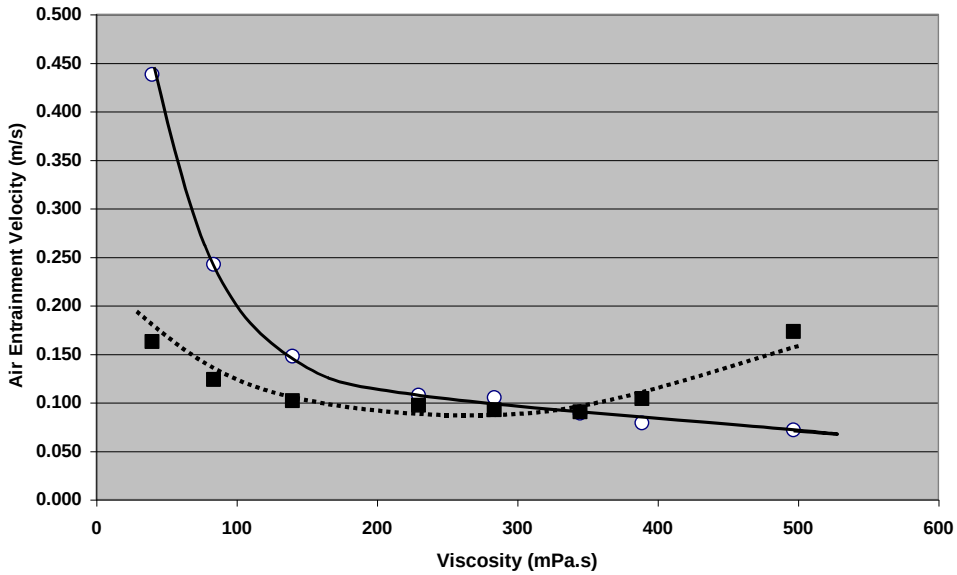

Figure 6: Air Entrainment Speed on the rough (■) and smooth sides (○) of Paper1 showing switch at a high critical viscosity.

Point (■) at 497 mPa.s did not appear by mistake in the initial version

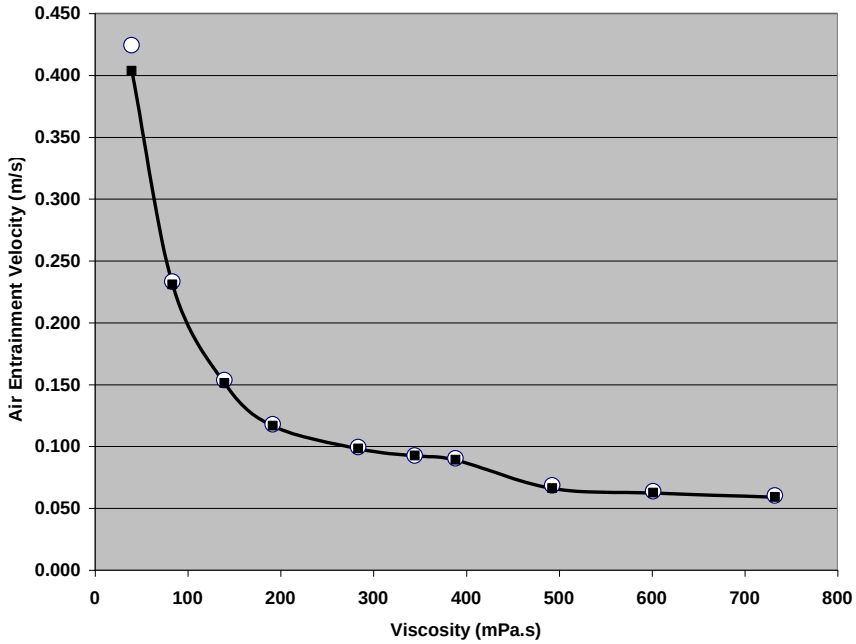

Figure 7: Air Entrainment Speed on the two sides of of Polyester1 showing no switch.

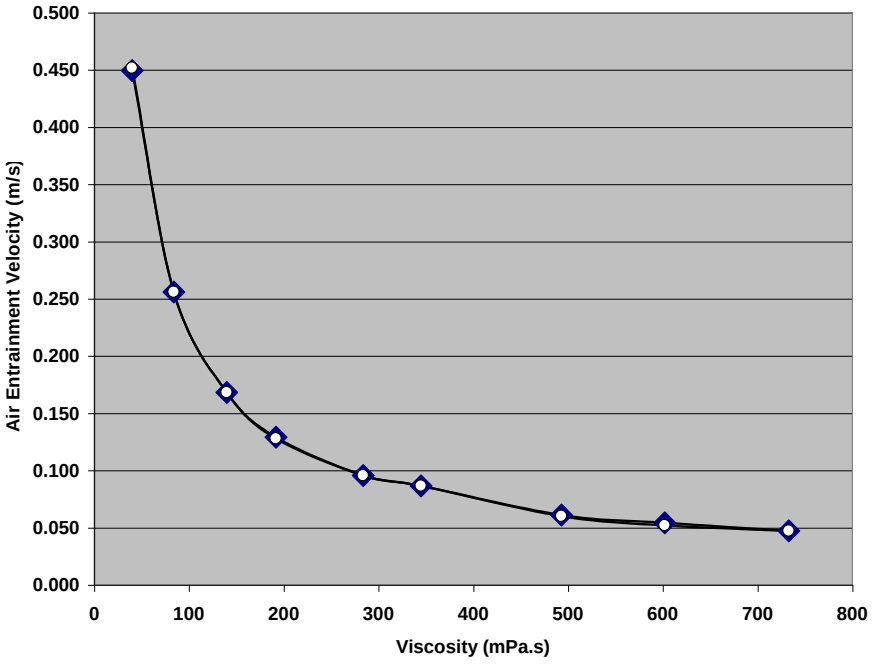

Figure 8: Air Entrainment Speed on the two sides of Polyester2 showing no switch.